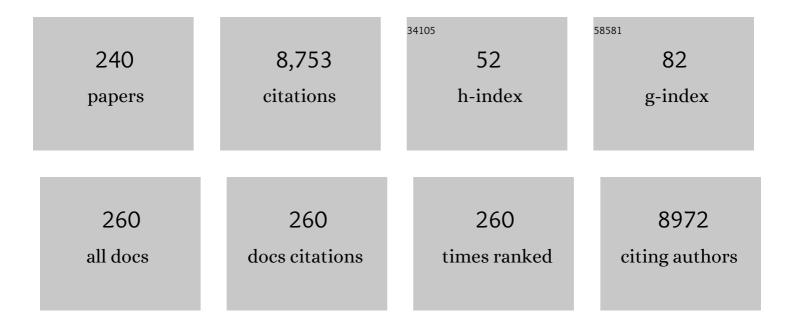
Daniel Chappard

List of Publications by Year in descending order

Source: https://exaly.com/author-pdf/5213440/publications.pdf Version: 2024-02-01



#	Article	IF	CITATIONS
1	Trabecular Bone Microarchitecture, Bone Mineral Density, and Vertebral Fractures in Male Osteoporosis. Journal of Bone and Mineral Research, 2000, 15, 13-19.	2.8	336
2	2-Hydroxyethyl Methacrylate (HEMA): Chemical Properties and Applications in Biomedical Fields. Journal of Macromolecular Science - Reviews in Macromolecular Chemistry and Physics, 1992, 32, 1-34.	2.2	332
3	Effects of Roughness, Fibronectin and Vitronectin on Attachment, Spreading, and Proliferation of Human Osteoblast-Like Cells (Saos-2) on Titanium Surfaces. Calcified Tissue International, 1999, 64, 499-507.	3.1	305
4	Recruitment of new osteoblasts and osteoclasts is the earliest critical event in the pathogenesis of human multiple myeloma Journal of Clinical Investigation, 1991, 88, 62-66.	8.2	222
5	Mechanisms of bone destruction in multiple myeloma: the importance of an unbalanced process in determining the severity of lytic bone disease Journal of Clinical Oncology, 1989, 7, 1909-1914.	1.6	218
6	Influence of fluoride, hydrogen peroxide and lactic acid on the corrosion resistance of commercially pure titanium. Acta Biomaterialia, 2006, 2, 121-129.	8.3	184
7	Altered trabecular architecture induced by Corticosteroids: A Bone Histomorphometric Study. Journal of Bone and Mineral Research, 1996, 11, 676-685.	2.8	168
8	Gamma irradiation of human bone allografts alters medullary lipids and releases toxic compounds for osteoblast-like cells. Biomaterials, 2000, 21, 369-376.	11.4	167
9	Comparison Insight Bone Measurements by Histomorphometry and μCT. Journal of Bone and Mineral Research, 2005, 20, 1177-1184.	2.8	166
10	Synchrotron X-ray microtomography (on a micron scale) provides three-dimensional imaging representation of bone ingrowth in calcium phosphate biomaterials. Biomaterials, 2003, 24, 4591-4601.	11.4	147
11	Trabecular bone microarchitecture: A review. Morphologie, 2008, 92, 162-170.	0.9	139
12	Bone loss and teeth. Joint Bone Spine, 2005, 72, 215-221.	1.6	117
13	Quantifiable excess of bone resorption in monoclonal gammopathy is an early symptom of malignancy: a prospective study of 87 bone biopsies. Blood, 1996, 87, 4762-4769.	1.4	113
14	Cancer-associated bone disease. Osteoporosis International, 2013, 24, 2929-2953.	3.1	113
15	Bone embedding in pure methyl methacrylate at low temperature preserves enzyme activities. Acta Histochemica, 1987, 81, 183-190.	1.8	105
16	Osteoclastic resorption of Ca-P biomaterials implanted in rabbit bone. Calcified Tissue International, 1993, 53, 348-356.	3.1	103
17	Comparative effects of five bisphosphonates on apoptosis of macrophage cells in vitro. Biochemical Pharmacology, 2007, 73, 718-723.	4.4	103
18	Image analysis measurements of roughness by texture and fractal analysis correlate with contact profilometry. Biomaterials, 2003, 24, 1399-1407.	11.4	102

#	Article	IF	CITATIONS
19	New laboratory tools in the assessment of bone quality. Osteoporosis International, 2011, 22, 2225-2240.	3.1	101

 $_{20}$ Effects of negatively charged groups (carboxymethyl) on the calcification of poly(2-hydroxyethyl) Tj ETQq0 0 0 rgBT /Qverlock 10 Tf 50 $\frac{1}{12}$

21	Texture analysis of X-ray radiographs is a more reliable descriptor of bone loss than mineral content in a rat model of localized disuse induced by the Clostridium botulinum toxin. Bone, 2001, 28, 72-79.	2.9	96
22	Pharmacologic inhibitors of lκB kinase suppress growth and migration of mammary carcinosarcoma cells <i>in vitro</i> and prevent osteolytic bone metastasis <i>in vivo</i> . Molecular Cancer Therapeutics, 2009, 8, 2339-2347.	4.1	94
23	Mechanisms of Bone Lesions in Multiple Myeloma. Hematology/Oncology Clinics of North America, 1992, 6, 285-295.	2.2	91
24	Glucose-dependent insulinotropic polypeptide (GIP) receptor deletion leads to reduced bone strength and quality. Bone, 2013, 56, 337-342.	2.9	89
25	Proliferation and differentiation of osteoblasts and adipocytes in rat bone marrow stromal cell cultures: Effects of dexamethasone and calcitriol. Journal of Cellular Biochemistry, 2003, 89, 364-372.	2.6	82
26	Optimal bone mechanical and material properties require a functional glucagon-like peptide-1 receptor. Journal of Endocrinology, 2013, 219, 59-68.	2.6	80
27	Embedding Iliac Bone Biopsies at Low Temperature using Glycol and Methyl Methacrylates. Biotechnic & Histochemistry, 1983, 58, 299-308.	0.4	79
28	Bone Mineral Density and Vertebral Fractures in Men. Osteoporosis International, 1999, 10, 265-270.	3.1	78
29	Fractal dimension of trabecular bone: comparison of three histomorphometric computed techniques for measuring the architectural two-dimensional complexity. Journal of Pathology, 2001, 195, 515-521.	4.5	77
30	Comparison of eight histomorphometric methods for measuring trabecular bone architecture by image analysis on histological sections. Microscopy Research and Technique, 1999, 45, 303-312.	2.2	75
31	Botulinum toxin in masticatory muscles of the adult rat induces bone loss at the condyle and alveolar regions of the mandible associated with a bone proliferation at a muscle enthesis. Bone, 2015, 77, 75-82.	2.9	74
32	Sinus lift augmentation and β-TCP: A microCT and histologic analysis on human bone biopsies. Micron, 2010, 41, 321-326.	2.2	71
33	Enhanced bone integration of implants with increased surface roughness: a long term study in the sheep. Journal of Dentistry, 2002, 30, 195-203.	4.1	70
34	Glucose-dependent insulinotropic polypeptide receptor deficiency leads to modifications of trabecular bone volume and quality in mice. Bone, 2013, 53, 221-230.	2.9	70
35	Texture analysis of X-ray radiographs of iliac bone is correlated with bone micro-CT. Osteoporosis International, 2006, 17, 447-454.	3.1	67
36	Respective roles of porto-septal fibrosis and centrilobular fibrosis in alcoholic liver disease. Journal of Pathology, 2003, 201, 55-62.	4.5	65

#	Article	IF	CITATIONS
37	Texture analysis of X-ray radiographs is correlated with bone histomorphometry. Journal of Bone and Mineral Metabolism, 2005, 23, 24-29.	2.7	65
38	Excessive bone resorption in human plasmacytomas: direct induction by tumour cells <i>in vivo</i> . British Journal of Haematology, 1995, 90, 721-724.	2.5	64
39	Biodegradability of poly (2-hydroxyethyl methacrylate) in the presence of the J774.2 macrophage cell line. Biomaterials, 2004, 25, 5155-5162.	11.4	61
40	Fat in bone xenografts: Importance of the purification procedures on cleanliness, wettability and biocompatibility. Biomaterials, 1993, 14, 507-512.	11.4	59
41	Free radicals and side products released during methylmethacrylate polymerization are cytotoxic for osteoblastic cells. , 1998, 40, 124-131.		59
42	Rat Models of Bone Metastases. Clinical and Experimental Metastasis, 2005, 22, 605-614.	3.3	59
43	Bone status in a mouse model of genetic hemochromatosis. Osteoporosis International, 2011, 22, 2313-2319.	3.1	58
44	Cutaneous manifestations in Hymenoptera and Diptera anaphylaxis: relationship with basal serum tryptase. Clinical and Experimental Allergy, 2009, 39, 717-725.	2.9	57
45	Importance of quantitative histology of bone changes in monoclonal gammopathy. British Journal of Cancer, 1986, 53, 805-810.	6.4	56
46	Cobalt, chromium and nickel affect hydroxyapatite crystal growth in vitro. Acta Biomaterialia, 2010, 6, 1555-1560.	8.3	56
47	Effects of the length of crosslink chain on poly(2-hydroxyethyl methacrylate) (pHEMA) swelling and biomechanical properties. Journal of Biomedical Materials Research - Part A, 2006, 77A, 35-42.	4.0	55
48	Histochemical identification of osteoclasts. Review of current methods and reappraisal of a simple procedure for routine diagnosis on undecalcified human iliac bone biopsies. Basic and Applied Histochemistry, 1983, 27, 75-85.	0.1	55
49	Alcoholic cirrhosis and osteoporosis in men: a light and scanning electron microscopy study Journal of Studies on Alcohol and Drugs, 1991, 52, 269-274.	2.3	54
50	Phenotypic effects of continuous or discontinuous treatment with dexamethasone and/or calcitriol on osteoblasts differentiated from rat bone marrow stromal cells. Journal of Cellular Biochemistry, 2002, 85, 640-650.	2.6	54
51	Synthesis of methacryloyloxyethyl phosphate copolymers and in vitro calcification capacity. Biomaterials, 2004, 25, 205-213.	11.4	54
52	Inflammatory reaction in rats muscle after implantation of biphasic calcium phosphate micro particles. Journal of Materials Science: Materials in Medicine, 2007, 18, 287-294.	3.6	54
53	Iron inhibits hydroxyapatite crystal growth in vitro. Metabolism: Clinical and Experimental, 2008, 57, 903-910.	3.4	54
54	Aluminum and bone: Review of new clinical circumstances associated with Al3+ deposition in the calcified matrix of bone. Morphologie, 2016, 100, 95-105.	0.9	54

#	Article	IF	CITATIONS
55	Cortical osteoclasts are less sensitive to etidronate than trabecular osteoclasts. Journal of Bone and Mineral Research, 1991, 6, 673-680.	2.8	53
56	Effects of a bisphosphonate (1-hydroxy ethylidene-1,1 bisphosphonic acid) on osteoclast number during prolonged bed rest in healthy humans. Metabolism: Clinical and Experimental, 1989, 38, 822-825.	3.4	52
57	Bone Microarchitecture and Bone Fragility in Men: DXA and Histomorphometry in Humans and in the Orchidectomized Rat Model. Calcified Tissue International, 2001, 69, 214-217.	3.1	52
58	Migration of metal and polyethylene particles from articular prostheses may generate lymphadenopathy with histiocytosis. , 1996, 30, 157-164.		51
59	Decreased Bone Formation Explains Osteoporosis in a Genetic Mouse Model of Hemochromatosiss. PLoS ONE, 2016, 11, e0148292.	2.5	51
60	Poly(2-hydroxy ethyl methacrylate)-alkaline phosphatase: A composite biomaterial allowing in vitro studies of bisphosphonates on the mineralization process. Journal of Biomaterials Science, Polymer Edition, 2000, 11, 849-868.	3.5	50
61	Fractal dimension can distinguish models and pharmacologic changes in liver fibrosis in rats. Hepatology, 2002, 36, 840-849.	7.3	48
62	Effects of FGF-2 release from a hydrogel polymer on bone mass and microarchitecture. Biomaterials, 2008, 29, 1593-1600.	11.4	48
63	Three-Dimensional Characterization of the Vascular Bed in Bone Metastasis of the Rat by Microcomputed Tomography (MicroCT). PLoS ONE, 2011, 6, e17336.	2.5	48
64	Adherence of osteoblast-like cells on calcospherites developed on a biomaterial combining poly(2-hydroxyethyl) methacrylate and alkaline phosphatase. Bone, 2002, 30, 152-158.	2.9	47
65	The early remodeling phases around titanium implants: a histomorphometric assessment of bone quality in a 3- and 6-month study in sheep. International Journal of Oral and Maxillofacial Implants, 1999, 14, 189-96.	1.4	47
66	Histologic evidence of an abnormal bone remodeling in b-cell malignancies other than multiple myeloma. Cancer, 1988, 62, 1163-1170.	4.1	44
67	Biomaterial porosity determined by fractal dimensions, succolarity and lacunarity on microcomputed tomographic images. Materials Science and Engineering C, 2013, 33, 2025-2030.	7.3	42
68	Increased bone remodeling due to ovariectomy dramatically increases tumoral growth in the 5T2 multiple myeloma mouse model. Bone, 2003, 33, 283-292.	2.9	41
69	Relationship Between Computed Tomographic Image Analysis and Histomorphometry for Microarchitectural Characterization of Human Calcaneus. Calcified Tissue International, 2004, 75, 23-31.	3.1	40
70	Bone Mass and Bone Quality Are Altered by Hypoactivity in the Chicken. PLoS ONE, 2015, 10, e0116763.	2.5	40
71	Quantifiable excess of bone resorption in monoclonal gammopathy is an early symptom of malignancy: a prospective study of 87 bone biopsies. Blood, 1996, 87, 4762-9.	1.4	40
72	Microâ€osteoclast resorption as a characteristic feature of Bâ€cell malignancies other than multiple myeloma. British Journal of Haematology, 1990, 76, 469-475.	2.5	39

#	Article	IF	CITATIONS
73	Bone metastasis: Histological changes and pathophysiological mechanisms in osteolytic or osteosclerotic localizations. A review. Morphologie, 2011, 95, 65-75.	0.9	37
74	Beneficial effects of a N-terminally modified GIP agonist on tissue-level bone material properties. Bone, 2014, 63, 61-68.	2.9	37
75	Vertebral fractures are associated with increased cortical porosity in iliac crest bone biopsy of men with idiopathic osteoporosis. Bone, 2009, 44, 413-417.	2.9	36
76	A non-steroidal anti-inflammatory drug (ketoprofen) does not delay β-TCP bone graft healing. Acta Biomaterialia, 2010, 6, 3310-3317.	8.3	36
77	Comparison of Histomorphometric Descriptors of Bone Architecture with Dual-Energy X-ray Absorptiometry for Assessing Bone Loss in the Orchidectomized Rat. Osteoporosis International, 2002, 13, 422-428.	3.1	35
78	Evaluation of an injectable bone substitute (βTCP/hydroxyapatite/hydroxy-propyl-methyl-cellulose) in severely osteopenic and aged rats. Journal of Biomedical Materials Research - Part A, 2006, 78A, 570-580.	4.0	35
79	Bone microarchitecture in males with corticosteroid-induced osteoporosis. Osteoporosis International, 2007, 18, 487-494.	3.1	35
80	Glucose-dependent insulinotropic polypeptide (GIP) directly affects collagen fibril diameter and collagen cross-linking in osteoblast cultures. Bone, 2015, 74, 29-36.	2.9	34
81	High fat-fed diabetic mice present with profound alterations of the osteocyte network. Bone, 2016, 90, 99-106.	2.9	34
82	Two dental implants designed for immediate loading: a finite element analysis. International Journal of Oral and Maxillofacial Implants, 2002, 17, 353-62.	1.4	34
83	Alteration of the bone tissue material properties in type 1 diabetes mellitus: A Fourier transform infrared microspectroscopy study. Bone, 2015, 76, 31-39.	2.9	33
84	The influence of processes for the purification of human bone allografts on the matrix surface and cytocompatibility. Biomaterials, 2006, 27, 4204-4211.	11.4	31
85	Disuse and orchidectomy have additional effects on bone loss in the aged male rat. Osteoporosis International, 2007, 18, 85-92.	3.1	31
86	Osteoclast cytomorphometry demonstrates an abnormal population in B cell malignancies but not in multiple myeloma. Calcified Tissue International, 1991, 48, 13-17.	3.1	30
87	Interactions between microenvironment and cancer cells in two animal models of bone metastasis. British Journal of Cancer, 2008, 98, 809-815.	6.4	30
88	Non-connected versus interconnected macroporosity in poly(2-hydroxyethyl methacrylate) polymers. An X-ray microtomographic and histomorphometric study. Journal of Biomaterials Science, Polymer Edition, 2002, 13, 1105-1117.	3.5	29
89	Sclerostin antibody reduces long bone fractures in the oim/oim model of osteogenesis imperfecta. Bone, 2019, 124, 137-147.	2.9	29
90	Shape and orientation of osteoblast-like cells (Saos-2) are influenced by collagen fibers in xenogenic bone biomaterial. , 1998, 40, 350-357.		28

#	Article	IF	CITATIONS
91	Trabecular bone microarchitecture is related to the number of risk factors and etiology in osteoporotic men. Microscopy Research and Technique, 2007, 70, 952-959.	2.2	28
92	Polystyrene scaffolds based on microfibers as a bone substitute; development and in vitro study. Acta Biomaterialia, 2016, 29, 380-388.	8.3	28
93	Bone mineralization and vascularization in bisphosphonate-related osteonecrosis of the jaw: an experimental study in the rat. Clinical Oral Investigations, 2018, 22, 2997-3006.	3.0	28
94	Polymerization of 2â€(hydroxyethyl)methacrylate by two different initiator/accelerator systems: a Raman spectroscopic monitoring. Journal of Raman Spectroscopy, 2008, 39, 767-771.	2.5	27
95	A new stable CIP–Oxyntomodulin hybrid peptide improved bone strength both at the organ and tissue levels in genetically-inherited type 2 diabetes mellitus. Bone, 2016, 87, 102-113.	2.9	27
96	Chemical structure of methylmethacrylate-2-[2′,3′,5′-triiodobenzoyl]oxoethyl methacrylate copolymer, radio-opacity, in vitro and in vivo biocompatibility. Acta Biomaterialia, 2008, 4, 1762-1769.	8.3	26
97	Reproducibility of CT-based bone texture parameters of cancellous calf bone samples: Influence of slice thickness. European Journal of Radiology, 2008, 67, 514-520.	2.6	26
98	Glucocorticoids reduce alveolar and trabecular bone in mice. Joint Bone Spine, 2013, 80, 77-81.	1.6	26
99	In vitro calcification of chemically functionalized carbon nanotubes. Acta Biomaterialia, 2010, 6, 4110-4117.	8.3	25
100	Spontaneous multiple vertebral fractures revealed primary haemochromatosis. Osteoporosis International, 1996, 6, 338-340.	3.1	24
101	Bone changes in myelofibrosis with myeloid metaplasia: a histomorphometric and microcomputed tomographic study. European Journal of Haematology, 2007, 78, 500-509.	2.2	24
102	Effect of alpha tocopherol acetate in Walker 256/B cells-induced oxidative damage in a rat model of breast cancer skeletal metastases. Chemico-Biological Interactions, 2009, 182, 98-105.	4.0	24
103	Biomaterial granules used for filling bone defects constitute 3D scaffolds: porosity, microarchitecture and molecular composition analyzed by microCT and Raman microspectroscopy. Journal of Biomedical Materials Research - Part B Applied Biomaterials, 2019, 107, 415-423.	3.4	24
104	Relations between Radiograph Texture Analysis and Microcomputed Tomography in Two Rat Models of Bone Metastases. Cells Tissues Organs, 2006, 182, 182-192.	2.3	23
105	Effects of risedronate in a rat model of osteopenia due to orchidectomy and disuse: Densitometric, histomorphometric and microtomographic studies. Micron, 2008, 39, 998-1007.	2.2	23
106	Micro and macroarchitectural changes at the tibia after botulinum toxin injection in the growing rat. Bone, 2012, 50, 858-864.	2.9	23
107	Bone grafts cultured with bone marrow stromal cells for the repair of critical bone defects: An experimental study in mice. Journal of Biomedical Materials Research - Part A, 2009, 90A, 1218-1229.	4.0	22
108	Simultaneous Identification of Calcified Cartilage, Bone and Osteoid Tissue on Plastic Sections: New Polychrome Procedures Specially Adapted to Image Analyzer Systems. Journal of Histotechnology, 1986, 9, 95-97.	0.5	21

#	Article	IF	CITATIONS
109	Evaluation of the Bone Status in High-Level Cyclists. Journal of Clinical Densitometry, 2012, 15, 103-107.	1.2	21
110	Comparison insight dual X-ray absorptiometry (DXA), histomorphometry, ash weight, and morphometric indices for bone evaluation in an animal model (the orchidectomized rat) of male osteoporosis. Calcified Tissue International, 2001, 68, 31-37.	3.1	20
111	Glucocorticoid-Induced Osteoporosis: A Review. Clinical Reviews in Bone and Mineral Metabolism, 2010, 8, 15-26.	0.8	20
112	Three-dimensional arrangement of \hat{l}^2 -tricalcium phosphate granules evaluated by microcomputed tomography and fractal analysis. Acta Biomaterialia, 2015, 11, 404-411.	8.3	20
113	Hypodynamia Alters Bone Quality and Trabecular Microarchitecture. Calcified Tissue International, 2017, 100, 332-340.	3.1	20
114	Spatial Distribution of Trabeculae in Iliac Bone from 145 Osteoporotic Females. Cells Tissues Organs, 1988, 132, 137-142.	2.3	19
115	Mandibular bone loss in an animal model of male osteoporosis (orchidectomized rat): a radiographic and densitometric study. Osteoporosis International, 2004, 15, 814-9.	3.1	19
116	<i>In vitro</i> kinetic study of growth and mineralization of osteoblastâ€like cells (Saosâ€2) on titanium surface coated with a RGD functionalized bisphosphonate. Journal of Biomedical Materials Research - Part B Applied Biomaterials, 2009, 90B, 873-881.	3.4	19
117	Strontium ranelate decreases the incidence of new caudal vertebral fractures in a growing mouse model with spontaneous fractures by improving bone microarchitecture. Osteoporosis International, 2011, 22, 289-297.	3.1	19
118	Plasma cells release membrane microparticles in a mouse model of multiple myeloma. Micron, 2013, 54-55, 75-81.	2.2	19
119	Repair of calvarial bone defects in mice using electrospun polystyrene scaffolds combined with β-TCP or gold nanoparticles. Micron, 2017, 93, 29-37.	2.2	19
120	The GLP-1 Receptor Agonist Exenatide Ameliorates Bone Composition and Tissue Material Properties in High Fat Fed Diabetic Mice. Frontiers in Endocrinology, 2019, 10, 51.	3.5	19
121	Aluminum Ingestion Promotes Colorectal Hypersensitivity in Rodents. Cellular and Molecular Gastroenterology and Hepatology, 2019, 7, 185-196.	4.5	19
122	Sclerostin-Antibody Treatment Decreases Fracture Rates in Axial Skeleton and Improves the Skeletal Phenotype in Growing oim/oim Mice. Calcified Tissue International, 2020, 106, 494-508.	3.1	19
123	Orchidectomy Models of Osteoporosis. Methods in Molecular Biology, 2008, 455, 125-134.	0.9	19
124	Disuse induced by botulinum toxin affects the bone marrow expression profile of bone genes leading to a rapid bone loss. Journal of Musculoskeletal Neuronal Interactions, 2013, 13, 27-36.	0.1	19
125	Medullar fat influences texture analysis of trabecular microarchitecture on X-ray radiographs. European Journal of Radiology, 2006, 58, 404-410.	2.6	18
126	Osteoblast-Like Cell Behavior on Porous Scaffolds Based on Poly(styrene) Fibers. BioMed Research International, 2014, 2014, 1-6.	1.9	18

#	Article	IF	CITATIONS
127	GIP analogues augment bone strength by modulating bone composition in diet-induced obesity in mice. Peptides, 2020, 125, 170207.	2.4	18
128	Does titanium surface treatment influence the bone-implant interface? SEM and histomorphometry in a 6-month sheep study. International Journal of Oral and Maxillofacial Implants, 1996, 11, 506-11.	1.4	18
129	Migration of polyethylene particles around nonloosened cemented femoral components from a total hip arthroplasty?an autopsy study. Journal of Biomedical Materials Research Part B, 2004, 69B, 205-215.	3.1	17
130	Ex vivo bone mineral density of the wrist: influence of medullar fat. Bone, 2004, 34, 1023-1028.	2.9	17
131	Bone mass and microarchitecture of irradiated and bone marrow-transplanted mice: influences of the donor strain. Osteoporosis International, 2009, 20, 435-443.	3.1	17
132	Thein vivocalcification capacity of a copolymer, based on methacryloyloxyethyl phosphate, does not favor osteoconduction. Journal of Biomedical Materials Research - Part A, 2004, 69A, 584-589.	4.0	16
133	Selection of a highly aggressive myeloma cell line by an altered bone microenvironment in the C57BL/KaLwRij mouse. Biochemical and Biophysical Research Communications, 2004, 316, 859-866.	2.1	16
134	Migration of wear debris of polyethylene depends on bone microarchitecture. Journal of Biomedical Materials Research - Part B Applied Biomaterials, 2009, 90B, 730-737.	3.4	16
135	The cathepsin K inhibitor AAE581 induces morphological changes in osteoclasts of treated patients. Microscopy Research and Technique, 2010, 73, 726-732.	2.2	16
136	Computed Microtomography of Bone Specimens for Rapid Analysis of Bone Changes Associated With Malignancy. Anatomical Record, 2010, 293, 1125-1133.	1.4	16
137	Mandibular bone effects of botulinum toxin injections in masticatory muscles in adult. Oral Surgery, Oral Medicine, Oral Pathology and Oral Radiology, 2020, 129, 100-108.	0.4	16
138	MICROCT AND PREPARATION OF ß-TCP GRANULAR MATERIAL BY THE POLYURETHANE FOAM METHOD. Image Analysis and Stereology, 2009, 28, 103.	0.9	16
139	Measurement by vertical scanning profilometry of resorption volume and lacunae depth caused by osteoclasts on dentine slices. Journal of Microscopy, 2011, 241, 147-152.	1.8	15
140	Depth and volume of resorption induced by osteoclasts generated in the presence of RANKL, TNF-alpha/IL-1 or LIGHT. Cytokine, 2012, 57, 294-299.	3.2	15
141	Relationships between bone mass and microâ€architecture at the mandible and iliac bone in edentulous subjects: a dual Xâ€ray absorptiometry, computerised tomography and microcomputed tomography study. Gerodontology, 2012, 29, e585-94.	2.0	15
142	The interface between nacre and bone after implantation in the sheep: a nanotomographic and Raman study. Journal of Raman Spectroscopy, 2014, 45, 558-564.	2.5	15
143	3D Porous Architecture of Stacks of β-TCP Granules Compared with That of Trabecular Bone: A microCT, Vector Analysis, and Compression Study. Frontiers in Endocrinology, 2015, 6, 161.	3.5	15
144	Aluminum and iron can be deposited in the calcified matrix of bone exostoses. Journal of Inorganic Biochemistry, 2015, 152, 174-179.	3.5	15

#	Article	IF	CITATIONS
145	Efficacy of targeting bone-specific GIP receptor in ovariectomy-induced bone loss. Journal of Endocrinology, 2018, 239, 215-227.	2.6	15
146	Osteolytic Bone Lesions in the 5T2 Multiple Myeloma Model: Radiographic, Scanning Electron Microscopic, and Microtomographic Studies. Journal of Histotechnology, 2001, 24, 81-86.	0.5	14
147	Quantification of Dendritic Cells and Osteoclasts in the Bone Marrow of Patients with Monoclonal Gammopathy. Pathology and Oncology Research, 2009, 15, 65-72.	1.9	14
148	Viability of osteocytes in bone autografts harvested for dental implantology. Biomedical Materials (Bristol), 2009, 4, 015012.	3.3	14
149	β-TCP granules mixed with reticulated hyaluronic acid induce an increase in bone apposition. Biomedical Materials (Bristol), 2014, 9, 015001.	3.3	14
150	Contrast enhancement with uranyl acetate allows quantitative analysis of the articular cartilage by microCT: Application to mandibular condyles in the BTX rat model of disuse. Micron, 2017, 97, 35-40.	2.2	14
151	Is transiliac bone biopsy a painful procedure?. Clinical Nephrology, 2012, 77, 97-104.	0.7	14
152	Comparison between quantitative X-ray imaging, dual energy X-ray absorptiometry and microCT in the assessment of bone mineral density in disuse-induced bone loss. Journal of Musculoskeletal Neuronal Interactions, 2015, 15, 42-52.	0.1	14
153	Increased Nucleolar Organizer Regions in Osteoclast Nuclei of Paget's Bone Disease. Bone, 1998, 22, 45-49.	2.9	13
154	Bone structure of the calcaneus: analysis with magnetic resonance imaging and correlation with histomorphometric study. Osteoporosis International, 2004, 15, 827-33.	3.1	13
155	Ultrastructural characteristics of glucocorticoid-induced osteoporosis. Osteoporosis International, 2009, 20, 1089-1092.	3.1	13
156	Maxillary Sinus Lift with Beta-Tricalcium Phosphate (β-TCP) in Edentulous Patients: A Nanotomographic and Raman Study. Calcified Tissue International, 2017, 101, 280-290.	3.1	13
157	Characterization of wear debris released from alumina-on-alumina hip prostheses: Analysis of retrieved femoral heads and peri-prosthetic tissues. Micron, 2018, 104, 89-94.	2.2	13
158	Polyhydroxyalkanoate (PHBV) fibers obtained by a wet spinning method: Good in vitro cytocompatibility but absence of in vivo biocompatibility when used as a bone graft. Morphologie, 2019, 103, 94-102.	0.9	12
159	Mechanisms of bone lesions in multiple myeloma. Hematology/Oncology Clinics of North America, 1992, 6, 285-95.	2.2	12
160	Evaluation of Surface Roughness of Hydrogels by Fractal Texture Analysis during Swelling. Langmuir, 2006, 22, 4843-4845.	3.5	11
161	Comparison of Pencil-, Fan-, and Cone-Beam Dual X-ray Absorptiometers for Evaluation of Bone Mineral Content in Excised Rat Bone. Journal of Clinical Densitometry, 2002, 5, 355-361.	1.2	10
162	Texture analysis of computed tomographic images in osteoporotic patients with sinus lift bone graft reconstruction. Clinical Oral Investigations, 2013, 17, 1267-1272.	3.0	10

#	Article	IF	CITATIONS
163	Aluminum inhibits the growth of hydroxyapatite crystals developed on a biomimetic methacrylic polymer. Journal of Trace Elements in Medicine and Biology, 2013, 27, 346-351.	3.0	10
164	Trabecular microarchitecture in established osteoporosis: Relationship between vertebrae, distal radius and calcaneus by X-ray imaging texture analysis. Orthopaedics and Traumatology: Surgery and Research, 2013, 99, 52-59.	2.0	10
165	Osteopontin is histochemically detected by the AgNOR acid-silver staining. Histology and Histopathology, 2008, 23, 469-78.	0.7	10
166	Lean, fat and bone masses are influenced by orchidectomy in the rat. A densitometric X-ray absorptiometric study. Journal of Musculoskeletal Neuronal Interactions, 2001, 1, 209-13.	0.1	10
167	Synthesis and use of pHEMA microbeads with human EA.hy 926 endothelial cells. Journal of Biomedical Materials Research - Part B Applied Biomaterials, 2009, 89B, 501-507.	3.4	9
168	Does milling one-piece titanium dental implants induce osteocyte and osteoclast changes?. Morphologie, 2011, 95, 51-59.	0.9	9
169	<i>In vitro</i> assessment of osteoblast and macrophage mobility in presence of βâ€TCP particles by videomicroscopy. Journal of Biomedical Materials Research - Part A, 2011, 96A, 108-115.	4.0	9
170	Diversity of bone matrix adhesion proteins modulates osteoblast attachment and organization of actin cytoskeleton. Morphologie, 2014, 98, 53-64.	0.9	9
171	Analysis of β-tricalcium phosphate granules prepared with different formulations by nano-computed tomography and scanning electron microscopy. Journal of Artificial Organs, 2015, 18, 338-345.	0.9	9
172	Incretin-based therapy for the treatment of bone fragility in diabetes mellitus. Peptides, 2018, 100, 108-113.	2.4	9
173	Long-Term Quantitative Evaluation of Muscle and Bone Wasting Induced by Botulinum Toxin in Mice Using Microcomputed Tomography. Calcified Tissue International, 2018, 102, 695-704.	3.1	9
174	Osteocyte staining with rhodamine in osteonecrosis and osteoarthritis of the femoral head. Microscopy Research and Technique, 2019, 82, 2072-2078.	2.2	9
175	Human macrophages and osteoclasts resorb β-tricalcium phosphate in vitro but not mouse macrophages. Micron, 2019, 125, 102730.	2.2	9
176	Computational fluid dynamics simulation from microCT stacks of commercial biomaterials usable for bone grafting. Micron, 2020, 133, 102861.	2.2	9
177	Isolation of osteoprogenitors from murine bone marrow by selection of CD11b negative cells. Cytotechnology, 2008, 58, 163-171.	1.6	8
178	Biomimetic potential of some methacrylateâ€based copolymers: A comparative study. Biopolymers, 2009, 91, 966-973.	2.4	8
179	Porosity imaged by a vector projection algorithm correlates with fractal dimension measured on 3D models obtained by microCT. Journal of Microscopy, 2015, 258, 24-30.	1.8	8
180	Effects of aluminum on cells and tissues. Morphologie, 2016, 100, 49-50.	0.9	8

#	Article	IF	CITATIONS
181	Cytomorphometry of osteoclasts. Medical Laboratory Sciences, 1989, 46, 363-6.	0.2	8
182	Practical Investigations of Radical Polymerization of Glycolmethacrylate as an Embedding Medium. Journal of Histotechnology, 1989, 12, 89-92.	0.5	7
183	Evolution of the bone-titanium interface on implants coated/noncoated with xenogeneic bone particles: Quantitative microscopic analysis. , 1996, 32, 175-180.		7
184	Scanning and Transmission Electron Microscopy of Poly 2-Hydroxyethyl Methacrylate-Based Biomaterials. Journal of Histotechnology, 1997, 20, 343-346.	0.5	7
185	Osteopontin is an argentophilic protein in the bone matrix and in cells of kidney convoluted tubules. Morphologie, 2007, 91, 180-185.	0.9	7
186	Fetuin and osteocalcin interact with calcospherite formation during the calcification process of poly(2â€hydroxyethylmethacrylate) <i>in vitro</i> : a Raman microspectroscopic monitoring. Journal of Raman Spectroscopy, 2009, 40, 1234-1239.	2.5	7
187	Raman spectroscopic analysis and imaging in two cases of benign cementoma: Comparison with dental and bone tissues. Journal of Raman Spectroscopy, 2020, 51, 1044-1055.	2.5	7
188	Aluminum Osteodystrophy and Celiac Disease. Calcified Tissue International, 2003, 74, 122-123.	3.1	6
189	Effects of Risedronate in Runx2 Overexpressing Mice, an Animal Model for Evaluation of Treatment Effects on Bone Quality and Fractures. Calcified Tissue International, 2011, 88, 464-475.	3.1	6
190	Technical aspects: how do we best prepare bone samples for proper histological analysis?. , 2015, , 111-120.		6
191	Maxillary sinus floor elevation using Beta-Tricalcium-Phosphate (beta-TCP) or natural bone: same inflammatory response. Journal of Materials Science: Materials in Medicine, 2019, 30, 97.	3.6	6
192	Osteoclast Cytomorphometry in Patients with Femoral Neck Fracture. Pathology Research and Practice, 1996, 192, 573-578.	2.3	5
193	Nuclear Organizer Regions (AgNORs) Staining on Undecalcified Bone Embedded in Resin: Light and TEM Methodologies. Journal of Histotechnology, 1996, 19, 27-32.	0.5	5
194	Photopolymerized 2-Hydroxyethylmethacrylate as a mounting medium preserving immunocytochemical reaction and nuclear counterstain. Biotechnic and Histochemistry, 1999, 74, 135-140.	1.3	5
195	Some Biomechanical and Histologic Characteristics of Early-Loaded Locking Pin and Expandable Implants: A Pilot Histologic Canine Study. Clinical Implant Dentistry and Related Research, 2004, 6, 33-39.	3.7	5
196	In vivo erosion of orthopedic screws prepared from nacre (mother of pearl). Orthopaedics and Traumatology: Surgery and Research, 2016, 102, 913-918.	2.0	5
197	Asymmetric bone remodeling in mandibular and maxillary tori. Clinical Oral Investigations, 2017, 21, 2781-2788.	3.0	5
198	Metaplastic woven bone in bone metastases: A Fourier-transform infrared analysis and imaging of bone quality (FTIR). Morphologie, 2018, 102, 69-77.	0.9	5

#	Article	IF	CITATIONS
199	Hyaluronic Acid Stimulates Osseointegration of β-TCP in Young and Old Ewes. Calcified Tissue International, 2019, 105, 487-496.	3.1	5
200	Bone lesions in systemic mastocytosis: Bone histomorphometry and histopathological mechanisms. Morphologie, 2020, 104, 97-108.	0.9	5
201	Wear debris released by hip prosthesis analysed by microcomputed tomography. Journal of Microscopy, 2021, 282, 13-20.	1.8	5
202	Microarchitecture of titanium cylinders obtained by additive manufacturing does not influence osseointegration in the sheep. International Journal of Energy Production and Management, 2021, 8, rbab021.	3.7	5
203	Tooth Extraction Locally Stimulates Proliferation of Multiple Myeloma in a Patient with Mandibular Localizations. Acta Haematologica, 2017, 138, 201-207.	1.4	5
204	A single pretreatment by zoledronic acid converts metastases from osteolytic to osteoblastic in the rat. Microscopy Research and Technique, 2010, 73, 733-740.	2.2	4
205	Beta-tricalcium phosphate and bone surgery: Editorial. Morphologie, 2017, 101, 111-112.	0.9	4
206	Giant cells and osteoclasts present in bone grafted with nacre differ by nuclear cytometry evaluated by texture analysis. Journal of Materials Science: Materials in Medicine, 2019, 30, 100.	3.6	4
207	Texture analysis of trabecular bone around RM-Pressfit cementless acetabulum in a series of 46 patients during a 5 year period. Orthopaedics and Traumatology: Surgery and Research, 2019, 105, 1283-1287.	2.0	4
208	GLP-2 administration in ovariectomized mice enhances collagen maturity but did not improve bone strength. Bone Reports, 2020, 12, 100251.	0.4	4
209	In vivo osseointegration and erosion of nacre screws in an animal model. Journal of Biomedical Materials Research - Part B Applied Biomaterials, 2021, 109, 780-788.	3.4	4
210	Histochemical identification of wear debris released by alumina-on-alumina hip prostheses in the periprosthetic tissues. Orthopaedics and Traumatology: Surgery and Research, 2021, 107, 102636.	2.0	4
211	Comparison of Osteoinduction by Autologous Bone and Biphasic Calcium Phosphate Ceramic in Goats. Key Engineering Materials, 2007, 330-332, 1063-1066.	0.4	3
212	Synthesis and characterisation of core–shell structures for orthopaedic surgery. Journal of Biomechanics, 2007, 40, 3349-3353.	2.1	3
213	Unwrapping microcomputed tomographic images for measuring cortical osteolytic lesions in the 5T2 murine model of myeloma treated by bisphosphonate. Micron, 2015, 68, 107-114.	2.2	3
214	Vector analysis of porosity evidences bone loss at the epiphysis in the BTX rat model of disuse osteoporosis. Journal of the Anatomical Society of India, 2016, 65, 3-8.	0.2	3
215	Microcomputed tomography (microCT) and histology of the mandibular canal in human and laboratory animals. Morphologie, 2018, 102, 263-275.	0.9	3
216	Osseointegration of two types of titanium cylinders with geometric or trabecular microarchitecture: A nanotomographic and histomorphometric study. Morphologie, 2022, 106, 80-91.	0.9	3

#	Article	IF	CITATIONS
217	Thiazolidinediones cause compaction of nuclear heterochromatin in the pluripotent mesenchymal cell line C3H10T1/2 when inducing an adipogenic phenotype. Analytical and Quantitative Cytopathology and Histopathology, 2013, 35, 85-94.	0.2	3
218	<scp>ABCC6</scp> deficiency and bone loss: A double benefit of etidronate for patient presenting with pseudoxanthoma elasticum?. Experimental Dermatology, 2022, 31, 1635-1637.	2.9	3
219	Texture Analyses of X-Ray Micrographs (Fractal Geometry and Run Length) are Better Predictors of Bone Loss than Mineral Content in a Rat Model of Localized Disuse Osteopenia. , 2002, , 171-180.		2
220	Postnatal growth defect in mice upon persistent Hoxa2 expression in the chondrogenic cell lineage. Differentiation, 2012, 83, 158-167.	1.9	2
221	Ceramic-on-ceramic bearing: Recent progress and solved controversies. Orthopaedics and Traumatology: Surgery and Research, 2021, 107, 102799.	2.0	2
222	Necrosis of the femoral head, X-ray microtomography (microCT) and histology of retrieved human femoral heads. Morphologie, 2021, 105, 134-142.	0.9	2
223	Fractal dimension can distinguish models and pharmacologic changes in liver fibrosis in rats. Hepatology, 2002, 36, 840-849.	7.3	1
224	Multiphasic Biomaterials: A Concept for Bone Substitutes Developed in the "Pays de la Loire". Key Engineering Materials, 2007, 361-363, -171.	0.4	1
225	New microscopies, biomaterials: Two new axes for Morphologie. Morphologie, 2016, 100, 187-188.	0.9	1
226	The contribution of Micro-CT to the evaluation of trabecular bone at the posterior part of the auricular surface in men. International Journal of Legal Medicine, 2018, 132, 1231-1239.	2.2	1
227	Microvascularization of the human central and peripheral nervous system: A new microcomputed tomography method. Morphologie, 2020, 104, 247-253.	0.9	1
228	Scanning and Transmission Electron Microscopy of Poly 2-Hydroxyethyl Methacrylate-Based Biomaterials. Journal of Histotechnology, 1997, 20, 343-346.	0.5	1
229	Bone grafted with β â€ᠯCP granules in the rabbit: A microcomputed tomographic, histologic, Raman microspectrometric, and Raman imaging study. Journal of Raman Spectroscopy, 2020, 51, 2435-2446.	2.5	1
230	Bone Architecture Measured by Fractal Dimension and Connectivity Indices is More Precociously Altered than Mineral Content in the Orchidectomized Rat. , 2002, , 161-170.		0
231	Technical Aspects. , 2010, , 201-209.		Ο
232	Micro-architecture trabéculaire dans l'ostéoporose confirméeÂ: relations entre vertèbres, radius distal et calcanéus au moyen de l'analyse de texture d'images radiographiques. Revue De Chirurgie Orthopedique Et Traumatologique, 2013, 99, 34-42.	0.0	0
233	Multiple myeloma and bone. Morphologie, 2015, 99, 29-30.	0.9	0
234	Érosion in vivo de vis orthopédiques préparées à partir de la nacre d'huître perlière. Revue De Chirurgie Orthopedique Et Traumatologique, 2016, 102, 657-662.	0.0	0

#	Article	IF	CITATIONS
235	A new editorial project for Morphologie. Morphologie, 2017, 101, 53-54.	0.9	0
236	The effects of botulinum injection on bone and cartilage of the mandibular condyle. American Journal of Orthodontics and Dentofacial Orthopedics, 2020, 157, 285.	1.7	0
237	Identification histochimique des débris d'usure libérés par les prothèses de hanche alumine-alumine dans les tissus périprothétiques. Revue De Chirurgie Orthopedique Et Traumatologique, 2021, 107, 19-25.	0.0	0
238	Aseptic osteonecrosis: From the rheumatologist to the surgeon. Morphologie, 2021, 105, 79.	0.9	0
239	Technical aspects. , 2022, , 93-104.		0
240	Analyse de la texture de l'os trabéculaire autour d'une cupule non cimentée RM Pressfit®Â: une sÃ(Orie de	0

Analyse de la texture de l'os trab©culaire autour d'une cupule non ciment©e RM Pressfit®À: une s©rie de 46Âcas sur une période de 5Âans. Revue De Chirurgie Orthopedique Et Traumatologique, 2019, 105, 844. 240